Transcriptional Profiling of Leukocytes in Critically Ill COVID19 Patients: Implications for Interferon Response and Coagulation

Sean E. Gill (sgill8@uwo.ca)
Western University https://orcid.org/0000-0003-4791-1576
Claudia C. dos Santos
University of Toronto
David B. O'Gorman
Western University
David E. Carter
Robarts Research Institute
Eric K. Patterson
London Health Sciences Centre
Marat Slessarev
Western University
Claudio Martin
Western University
Mark Daley
Western University
Michael R. Miller
Western University
Gediminas Cepinskas
Western University
Douglas D. Fraser
Western University

Research

Keywords: COVID19, RNAseq, Leukocyte Transcriptome

Posted Date: November 16th, 2020

DOI: https://doi.org/10.21203/rs.3.rs-63632/v2

Version of Record: A version of this preprint was published on December 11th, 2020. See the published version at https://doi.org/10.1186/s40635-020-00361-9.

Abstract

Background: COVID19 is caused by the SARS-CoV-2 virus and has been associated with severe inflammation leading to organ dysfunction and mortality. Our aim was to profile the transcriptome in leukocytes from critically ill patients positive for COVID19 compared to those negative for COVID19 to better understand the COVID19 associated host response. For these studies, all patients admitted to our tertiary care intensive care unit (ICU) suspected of being infected with SARS-CoV-2, using standardized hospital screening methodologies, had blood samples collected at the time of admission to the ICU. Transcriptome profiling of leukocytes via ribonucleic acid sequencing (RNAseq) was then performed and differentially expressed genes as well as significantly enriched gene sets were identified.

Results: We enrolled seven COVID19+ (PCR positive, 2 SARS-CoV-2 genes) and seven age- and sex-matched COVID19- (PCR negative) control ICU patients. Cohorts were well-balanced with the exception that COVID19- patients had significantly higher total white blood cell counts and circulating neutrophils and COVID19+ patients were more likely to suffer bilateral pneumonia. The mortality rate for this cohort of COVID19+ ICU patients was 29%. As indicated by both single-gene based and gene set (GSEA) approaches, the major disease-specific transcriptional responses of leukocytes in critically ill COVID19+ ICU patients were: (i) a robust overrepresentation of interferon related gene expression; (ii) a marked decrease in the transcriptional level of genes contributing to general protein synthesis and bioenergy metabolism; and (iii) the dysregulated expression of genes associated with coagulation, platelet function, complement activation, and tumour necrosis factor/interleukin 6 signalling.

Conclusions: Our findings demonstrate that critically ill COVID19+ patients on day 1 of admission to the ICU display a unique leukocyte transcriptional profile that distinguishes them from COVID19- patients, providing guidance for future targeted studies exploring novel prognostic and therapeutic aspects of COVID19.

Introduction

Coronavirus Disease (COVID) 19 is continuing to spread rapidly throughout the world, negatively impacting infected individuals, the health systems that support them and the global economy. The novel coronavirus that causes COVID19, SARS-CoV-2, was zoonotically derived from the Wuhan region, in Hubei Province, China in late 2019 (1, 2). Patients infected with SARS-CoV-2 exhibit a range of symptoms from mild hypoxemia with preserved lung compliance, and a mild inflammatory response, to severe hypoxemia associated with loss of lung function and a dysregulated inflammatory response with sustained tumour necrosis factor (TNF) and serine proteases that typically necessitates admission to an intensive care unit (ICU) (3-6). The overall mortality rate of individuals with COVID19 has been reported to be approximately 3.4%; however, once COVID19 patients are admitted to the ICU, their mortality rate approximates 31-40% with a median of 9 days to ICU death (5-8).

Early reports have suggested that a dysregulated cytokine response drives the severity of organ injury and dysfunction in COVID19 patients who require life support (5, 9, 10). Transcriptional profiling of whole blood from these patients indicate an early and dynamic inflammatory response with enhanced expression of interleukin 1β (IL1β) associated genes and T cell activation (11). However, these observations were made in comparison to healthy controls, and the increased circulating levels of pro-inflammatory cytokines observed in patients with COVID19 are also observed in other forms of sepsis and acute respiratory distress syndrome (ARDS) (4, 10). Our aim was to transcriptionally profile COVID19 positive (COVID19+) ICU patients in comparison to COVID19 negative (COVID19-) ICU patients with severe acute respiratory diseases/conditions (5-7) .

Methods

Study participants and clinical data: This study was approved by the Human Subject Research Ethics Board at Western University (5-7). Patients who were admitted to our academic ICU and suspected of having COVID19 based on standard hospital screening procedures and who had acute non-cardiogenic hypoxic respiratory failure requiring mechanical ventilation > 48h were consecutively enrolled in the study. Patients were than separated into cohorts, either COVID19+ or COVID19-, based on detection of two SARS-CoV-2 viral genes using polymerase chain reaction (PCR). Patient baseline characteristics were recorded on admission and included age, sex, severity of illness scores, comorbidities, hematologic labs, creatinine, arterial partial pressure to inspired oxygen (P/F) ratio, chest x-ray findings and sepsis diagnosis using Sepsis 3.0 criteria (12). Clinical interventions received in the ICU included use of antibiotics, anti-viral agents, systemic corticosteroids, vasoactive medications, renal replacement therapy, high flow oxygen therapy, and mechanical ventilation (invasive and non-invasive). Final participant groups were constructed by identifying 7 COVID19+ patients and then matching to 7 COVID19- patients by age and sex only (5-7). These patients have been included in previous studies performed by our group and this is a retrospective evaluation of the biological data from these patients (5-7). Further, given the exploratory nature of the study, no sample size calculation was performed.

Blood draws: Blood was collected from patients upon ICU admission using standard operating procedures to ensure all samples were treated rapidly and equally (5-7). Blood was obtained via indwelling catheters and placed immediately on ice. Once transferred to a negative pressure hood, the blood was centrifuged and the buffy coat was isolated, aliquoted at 250 µl and frozen at -80°C. All samples were stored frozen in the Translational Research Centre, London, Ontario (directed by Dr. D.D. Fraser; https://translationalresearchcentre.com/) until use and freeze/thaw cycles were avoided (13, 14).

RNA isolation: Buffy coat cells were homogenized in Trizol LS and centrifuged at 12,000 rcf to remove cell debris. Following chloroform extraction, RNA was isolated using the RNeasy Micro Plus Kit (Qiagen) according to the manufacturer's protocol.

Illumina NextSeq Next Generation Sequencing: All samples were sequenced at the London Regional Genomics Centre (Robarts Research Institute, London, Ontario, Canada; http://www.lrgc.ca) using the Illumina NextSeq 500 (Illumina Inc., San Diego, CA).

Total RNA samples were quantified using the NanoDrop (Thermo Fisher Scientific, Waltham, MA) and quality was assessed using the Agilent 2100 Bioanalyzer (Agilent Technologies Inc., Palo Alto, CA) and the RNA 6000 Nano kit (Caliper Life Sciences, Mountain View, CA). Only samples with an RNA integrity number ≥ 6.0 were used. The samples were then processed using the Vazyme VAHTS Total RNA-seq (H/M/R) Library Prep Kit for Illumina (Vazyme, Nanjing, China) which includes ribosomal RNA (rRNA) reduction.

Briefly, samples were rRNA depleted, fragmented, and utilized for cDNA synthesis and PCR amplification with indexed primers to permit equimolar pooling of samples into one library. The pooled library size distribution was assessed on an Agilent High Sensitivity DNA Bioanalyzer chip, and quantitated using the Qubit 2.0 Fluorometer. (Thermo Fisher Scientific, Waltham, MA).

The library was sequenced on the Illumina NextSeq 500 as single end runs, 1 x76 bp, using High Output v2 kits (75 cycles). Fastq data files were analyzed using Partek Flow (St. Louis, MO; Suppl. Fig. 1). After importation, the data were aligned to the *Homo sapiens* genome hg19 using STAR 2.7.3a and annotated using RefSeq Transcripts 93. Features with more than 18 reads were normalized using Trimmed Mean of M-values (TMM) (https://doi.org/10.1186/gb-2010-11-3-r25) followed by adding 0.0001. Any batch effect due to the run date was removed using Partek Flow's Remove batch effect tool based on the results of the PCA plot and a dissimilarity plot analysis (Fig. 1A and Suppl. Fig. 2). The gene-specific analysis (GSA) function of Partek Flow was then used to determine differential gene expression in COVID19+ vs. COVID19- patients using Akaike Information Criteria corrected (AICc) – a repeated measure analysis using mixed models methodology. The filtered gene list (fold change of 1.5 and FDR p value > 0.0545) was then submitted to Metascape (https://metascape.org/gp/index.html#/main/step1) using express analysis of *H. sapiens* gene IDs (15). A subset of enriched terms were selected and rendered as a network plot, where terms with a similarity > 0.3 were connected by edges. Terms with the lowest p-values from each of the 20 clusters were selected, with the constraint that there are no more than 15 terms per cluster and no more than 250 terms in total. The network was visualized using Metascape, where each node represented an enriched term and was colored first by cluster ID and then by p-value. The filtered gene list was also analyzed for enriched KEGG pathway terms.

***Gene Set Enrichment Analysis (GSEA)*:** Functional enrichment of the cumulative changes in gene expression across *a priori* defined gene sets was performed in GSEA to avoid the limitations of single-gene differential gene expression methods (16). All 14,810 genes that passed quality control were included in this analysis. The MSigDB collection was used to perform three main enrichment analyses: (i) Hallmark gene set (50 gene sets containing overlaps between MSigDB collections that display coordinate expression); (ii) Canonical Pathways (C2, 2232 gene sets); and (iii) regulatory target gene sets (C3, transcription factors, 1137 gene sets) (17). The gene sets included in the analysis were limited to those

that contained between 10 and 500 genes. Permutation was conducted 1,000 times according to default-weighted enrichment statistics and by using a signal-to-noise metric to rank genes according to their differential expression levels across the COVID19+ vs. COVID19- groups. Significant gene sets were defined as those with an FDR ≤ 0.1. Visualization and network analyses were performed using the EnrichmentMap application for Cytoscape 3.8.0 (https://cytoscape.org/) according to default parameters (18). To determine the degree of similarity between gene sets (nodes), the combined coefficient using a merged version of the jacquard and overlap similarity coefficients was used to define edges (i.e., connecting lines) between the nodes (cut-off 0.375).

Population Statistics: Medians (IQRs) and frequency (%) were utilized to describe patient baseline characteristics for continuous and categorical variables, respectively. Continuous variables were compared using two-tailed Mann-Whitney U or Kruskal-Wallis tests, as appropriate. Categorical variables were compared using Fisher's exact test. SPSS version 26 (IBM Corp., Armonk, NY, USA) was used to perform all population statistics and p-values <0.05 were considered statistically significant.

Results

We profiled the leukocyte transcriptome of 7 COVID19+ ICU patients (median years of age=60.0, IQR= 56.0, 67.0) and 7 age- and sex-matched COVID19- ICU patients (median years of age=60.0, IQR=53.0, 63.0; P=0.520) on day 1 of admission to the ICU. Baseline demographic characteristics, comorbidities, laboratory values, and chest x-ray findings are reported in Table 1. Compared to the COVID19+, COVID19- ICU patients were more likely to have an increased white blood cell count, specifically neutrophils; however, COVID19+ ICU patients were more likely to have bilateral pneumonias. While SARS-CoV-2 was confirmed by PCR in 100% of COVID19+ ICU patients, an infectious agent was identified in 43% of COVID19- ICU patients and an infectious agent was 'suspected' in the remaining 57%. The mortality rate was 29% for COVID19+ ICU patients.

Principal components analysis revealed clustering of samples based on SARS-CoV-2 PCR status, suggesting that changes in gene expression in circulating leukocytes in COVID19+ patients were unique to SARS-CoV-2, rather than common to sepsis or/and ARDS in critically ill COVID19- patients (Fig. 1A). GSA yielded 1,311 differentially expressed genes (False Discovery Rate < 0.055 and a > 1.5-fold change; Suppl. Table 1), 254 of which were upregulated and 1057 were downregulated (Fig. 1B and 1C) in the circulating immune cells of COVID19+ patients.

Functional enrichment analysis performed in Enrichr (https://maayanlab.cloud/Enrichr/) suggested an overrepresentation of genes that characterize CD14+ monocytes and CD33+ myeloid cells (Suppl. Table 2) in COVID19+ patients. Further functional analysis using Metascape (Fig. 2) revealed an overall upregulation in IFN mediated gene transcription in leukocytes of COVID19+ ICU patients, whereas genes associated with protein translation were all downregulated in the leukocytes of COVID19+ relative to COVID19- ICU patients (Fig. 3). These findings were independently confirmed using an alternative analysis tool, Reactome (Suppl. Fig. 3), indicating highly reproducible responses.

GSEA was then used to identify differentially expressed gene sets in the entire data set. After correcting for multiple comparisons, GSEA revealed that about 68.5% of genes were decreased compared to 31.5% that were increased in COVID compared to non-COVID patients. Furthermore, a total of 7/50 gene sets were negatively enriched while 26/50 were positively enriched (FDR<10%). In addition to overrepresentation of genes associated with IFN signalling (Fig. 4), GSEA identified enrichment for gene sets involved in TNF and IL6 signalling, complement signalling, apoptosis, and coagulation pathways in COVID19+ ICU patients (Fig. 4). In contrast, gene transcripts contributing to metabolic pathways involving protein synthesis, oxidative phosphorylation, and DNA repair were consistently and markedly downregulated in COVID19+ ICU patients (Fig. 4). GSEA was also used to identify enrichment of specific transcription factor (TF) binding sites in the leukocytes of COVID19+ relative to COVID19- ICU patients that may shed light on the observed disease-associated modifications of leukocyte transcriptomes. Network analysis confirmed an over-representation of genes that shared cis-regulatory sequences for serum response factor (SRF), E2F/1, nuclear factor kappa beta (NFκB), and cAMP response element-binding protein (CREB) in the COVID19+ data set (Suppl Fig. 4).

EnrichmentMap and the Autoannotate function in Cytoscape 3.8.0 was used to perform network analyses to visualize higher level changes in biological organization. This approach identifies tightly connected nodes, or clusters, indicating shared relationships between differentially expressed genes (shared gene membership). We used an FDR cut-off of ≤ 0.1 and a nominal p-value of ≤ 0.01 to select genes sets for network analysis. Figure 5 highlights the top network clusters and key biological processes that were differentially regulated in COVID19+ vs. COVID19- ICU patients. Notable clusters/processes identified as being either positively or negatively enriched in COVID19+ ICU patients by these analyses included platelet activation (20 gene sets), neurotrophin signalling (29 gene sets), SUMOylation and ubiquitination of proteins (27 gene sets), and toll receptor cascades (12 gene sets).

Discussion

We profiled the leukocyte transcriptome of 7 COVID19+ ICU patients (median years of age=60.0, IQR= 56.0, 67.0) and 7 age- and sex-matched COVID19- ICU patients (median years of age=60.0, IQR=53.0, 63.0; P=0.520) on day 1 of admission to the ICU. Baseline demographic characteristics, comorbidities, laboratory values, and chest x-ray findings are reported in Table 1. Compared to the COVID19+, COVID19- ICU patients were more likely to have an increased white blood cell count, specifically neutrophils; however, COVID19+ ICU patients were more likely to have bilateral pneumonias. While SARS-CoV-2 was confirmed by PCR in 100% of COVID19+ ICU patients, an infectious agent was identified in 43% of COVID19- ICU patients and an infectious agent was 'suspected' in the remaining 57%. The mortality rate was 29% for COVID19+ ICU patients.

Principal components analysis revealed clustering of samples based on SARS-CoV-2 PCR status, suggesting that changes in gene expression in circulating leukocytes in COVID19+ patients were unique to SARS-CoV-2, rather than common to sepsis or/and ARDS in critically ill COVID19- patients (Fig. 1A). GSA yielded 1,311 differentially expressed genes (False Discovery Rate < 0.055 and a > 1.5-fold change;

Suppl. Table 1), 254 of which were upregulated and 1057 were downregulated (Fig. 1B and 1C) in the circulating immune cells of COVID19+ patients.

Functional enrichment analysis performed in Enrichr (https://maayanlab.cloud/Enrichr/) suggested an overrepresentation of genes that characterize CD14+ monocytes and CD33+ myeloid cells (Suppl. Table 2) in COVID19+ patients. Further functional analysis using Metascape (Fig. 2) revealed an overall upregulation in IFN mediated gene transcription in leukocytes of COVID19+ ICU patients, whereas genes associated with protein translation were all downregulated in the leukocytes of COVID19+ relative to COVID19- ICU patients (Fig. 3). These findings were independently confirmed using an alternative analysis tool, Reactome (Suppl. Fig. 3), indicating highly reproducible responses.

GSEA was then used to identify differentially expressed gene sets in the entire data set. After correcting for multiple comparisons, GSEA revealed that about 68.5% of genes were decreased compared to 31.5% that were increased in COVID compared to non-COVID patients. Furthermore, a total of 7/50 gene sets were negatively enriched while 26/50 were positively enriched (FDR<10%). In addition to overrepresentation of genes associated with IFN signalling (Fig. 4), GSEA identified enrichment for gene sets involved in TNF and IL6 signalling, complement signalling, apoptosis, and coagulation pathways in COVID19+ ICU patients (Fig. 4). In contrast, gene transcripts contributing to metabolic pathways involving protein synthesis, oxidative phosphorylation, and DNA repair were consistently and markedly downregulated in COVID19+ ICU patients (Fig. 4). GSEA was also used to identify enrichment of specific transcription factor (TF) binding sites in the leukocytes of COVID19+ relative to COVID19- ICU patients that may shed light on the observed disease-associated modifications of leukocyte transcriptomes. Network analysis confirmed an over-representation of genes that shared cis-regulatory sequences for serum response factor (SRF), E2F/1, nuclear factor kappa beta (NFκB), and cAMP response element-binding protein (CREB) in the COVID19+ data set (Suppl Fig. 4).

EnrichmentMap and the Autoannotate function in Cytoscape 3.8.0 was used to perform network analyses to visualize higher level changes in biological organization. This approach identifies tightly connected nodes, or clusters, indicating shared relationships between differentially expressed genes (shared gene membership). We used an FDR cut-off of ≤ 0.1 and a nominal p-value of ≤ 0.01 to select genes sets for network analysis. Figure 5 highlights the top network clusters and key biological processes that were differentially regulated in COVID19+ vs. COVID19- ICU patients. Notable clusters/processes identified as being either positively or negatively enriched in COVID19+ ICU patients by these analyses included platelet activation (20 gene sets), neurotrophin signalling (29 gene sets), SUMOylation and ubiquitination of proteins (27 gene sets), and toll receptor cascades (12 gene sets).

Conclusion

In summary, we report a unique transcriptome in COVID19+ ICU patients that can be distinguished from those of COVID19- patients despite the heterogeneity and timing of presentation/admission to the ICU. This unique transcriptome, which can be measured using common laboratory techniques suggesting it

may be amenable to future point-of-care tests, is driven by enhanced IFN signalling, dysregulated protein synthesis, and increased platelet activation and coagulation. Finally, given the significant impact of COVID19 critical illness on society, our novel data may provide guidance in future targeted studies exploring therapeutics in parallel with validation of our findings in larger COVID19+ cohorts.

Declarations

Ethics approval and consent to participate: This study was approved by the Human Subject Research Ethics Board at Western University.

Consent for publication: Not applicable.

Availability of data and materials: The datasets generated and/or analyzed during the current study are available in the GEO repository (Accession #: GSE154998), https://www.ncbi.nlm.nih.gov/geo/query/acc.cgi?acc=GSE154998. Datasets are also available from the corresponding author upon reasonable request.

Competing interests: The authors declare that they have no competing interests.

Funding: We acknowledge funding from Western University (Research), the Departments of Medicine and Pediatrics at Western University, the Lawson Health Research Institute (https://www.lawsonresearch.ca/), the London Health Sciences Foundation (https://lhsf.ca/), and the AMOSO Innovation Fund.

Authors' contributions: DDF, SEG, and DBO designed the research question. SEG and EKP isolated the leukocyte RNA. DEC performed the Next Generation Sequencing and individual gene analysis using Partek Flow, and CCD performed the Gene Set Enrichment Analysis. MRM performed the population statistics. SEG, CCD, DBO, DEC, GC, and DDF were major contributors in data analysis and writing the manuscript. MS, CM, and MD were involved in overall data analysis. All authors read and approved the final manuscript.

Acknowledgements: We thank the entire Lawson COVID19 Study Team for their support and hard work (Dr. Robert Arntfield, Dr. Ian Ball, Mr. Gordon Barkwell, Ms. Tracey Bentall, Dr. Karen Bosma, Ms. Saoirse Cameron, Ms. Eileen Campbell, Dr. Carolina Gillio-Meina, Dr. Robert Hegele, Ms. Natalya Odoardi, Dr. Ram Singh, Dr. Kelly Summers and Ms. Sue Tereschyn). We are grateful for the continuous assistance of the frontline Critical Care Nursing Staff at London Health Sciences Centre.

References

1. Huang C, Wang Y, Li X, et al.: Clinical features of patients infected with 2019 novel coronavirus in Wuhan, China. *The Lancet* 2020; 395:497–506
2. Zhou F, Yu T, Du R, et al.: Clinical course and risk factors for mortality of adult inpatients with COVID-19 in Wuhan, China: a retrospective cohort study. *Lancet* 2020; 395:1054–1062

3. Gattinoni L, Coppola S, Cressoni M, et al.: COVID-19 Does Not Lead to a “Typical” Acute Respiratory Distress Syndrome. *Am J Respir Crit Care Med* 2020; 201:1299–1300
4. McGonagle D, Sharif K, O'Regan A, et al.: The Role of Cytokines including Interleukin-6 in COVID-19 induced Pneumonia and Macrophage Activation Syndrome-Like Disease. *Autoimmun Rev* 2020; 102537
5. Fraser DD, Cepinskas G, Slessarev M, et al.: Inflammation Profiling of Critically Ill Coronavirus Disease 2019 Patients. *Critical Care Explorations* 2020; 2:e0144–8
6. Fraser DD, Cepinskas G, Patterson EK, et al.: Novel Outcome Biomarkers Identified with Targeted Proteomics of Plasma Obtained from Critically Ill COVID-19 Patients. *Critical Care Explorations* 2020;
7. Fraser DD, Patterson EK, Slessarev M, et al.: Endothelial Injury and Glycocalyx Degradation in Critically Ill COVID19 Patients: Implications for Microvascular Platelet Aggregation. *Critical Care Explorations* 2020;
8. Auld SC, Caridi-Scheible M, Blum JM, et al.: ICU and Ventilator Mortality Among Critically Ill Adults With Coronavirus Disease 2019. *Crit Care Med* 2020; Publish Ahead of Print
9. Mehta P, McAuley DF, Brown M, et al.: COVID-19: consider cytokine storm syndromes and immunosuppression. *The Lancet* 2020; 395:1033–1034
10. Chen X, Zhao B, Qu Y, et al.: Detectable serum SARS-CoV-2 viral load (RNAaemia) is closely correlated with drastically elevated interleukin 6 (IL-6) level in critically ill COVID-19 patients. *Clin Infect Dis* 2020; 9:3
11. Ong EZ, Chan YFZ, Leong WY, et al.: A Dynamic Immune Response Shapes COVID-19 Progression. *Cell Host and Microbe* 2020; 27:879–882.e2
12. Singer M, Deutschman CS, Seymour CW, et al.: The Third International Consensus Definitions for Sepsis and Septic Shock (Sepsis-3). *JAMA* 2016; 315:801–810
13. Brisson AR, Matsui D, Rieder MJ, et al.: Translational research in pediatrics: tissue sampling and biobanking. *Pediatrics* 2012; 129:153–162
14. Gillio-Meina C, Cepinskas G, Cecchini EL, et al.: Translational research in pediatrics II: blood collection, processing, shipping, and storage. *Pediatrics* 2013; 131:754–766
15. Zhou Y, Zhou B, Pache L, et al.: Metascape provides a biologist-oriented resource for the analysis of systems-level datasets. *Nat Commun* 2019; 10:1523–10
16. Subramanian A, Tamayo P, Mootha VK, et al.: Gene set enrichment analysis: a knowledge-based approach for interpreting genome-wide expression profiles. *Proceedings of the National Academy of Sciences* 2005; 102:15545–15550
17. Liberzon A, Subramanian A, Pinchback R, et al.: Molecular signatures database (MSigDB) 3.0. *Bioinformatics* 2011; 27:1739–1740
18. Shannon P, Markiel A, Ozier O, et al.: Cytoscape: a software environment for integrated models of biomolecular interaction networks. *Genome Research* 2003; 13:2498–2504

19. Angus DC: Management of sepsis: a 47-year-old woman with an indwelling intravenous catheter and sepsis. *JAMA* 2011; 305:1469–1477
20. Blanco-Melo D, Nilsson-Payant BE, Liu W-C, et al.: Imbalanced Host Response to SARS-CoV-2 Drives Development of COVID-19. *Cell* 2020; 181:1036–1045.e9
21. Schneider WM, Chevillotte MD, Rice CM: Interferon-stimulated genes: a complex web of host defenses. *Annu Rev Immunol* 2014; 32:513–545
22. Schindler C, Levy DE, Decker T: JAK-STAT signaling: from interferons to cytokines. *Journal of Biological Chemistry* 2007; 282:20059–20063
23. Zhang K, Kumar R: Interferon-alpha inhibits cyclin E- and cyclin D1-dependent CDK-2 kinase activity associated with RB protein and E2F in Daudi cells. *Biochem Biophys Res Commun* 1994; 200:522–528
24. Dagenais-Lussier X, Loucif H, Murira A, et al.: Sustained IFN-I Expression during Established Persistent Viral Infection: A “Bad Seed” for Protective Immunity. *Viruses* 2017; 10:12
25. Zagury D, Lachgar A, Chams V, et al.: Interferon alpha and Tat involvement in the immunosuppression of uninfected T cells and C-C chemokine decline in AIDS. *Proceedings of the National Academy of Sciences* 1998; 95:3851–3856
26. Le Saout C, Hasley RB, Imamichi H, et al.: Chronic exposure to type-I IFN under lymphopenic conditions alters CD4 T cell homeostasis. *PLoS Pathog* 2014; 10:e1003976
27. Merad M, Martin JC: Pathological inflammation in patients with COVID-19: a key role for monocytes and macrophages. *Nat Rev Immunol* 2020; 20:355–362
28. Lerkvaleekul B, Vilaiyuk S: Macrophage activation syndrome: early diagnosis is key. *Open Access Rheumatol* 2018; 10:117–128
29. Crayne CB, Albeituni S, Nichols KE, et al.: The Immunology of Macrophage Activation Syndrome. *Front Immunol* 2019; 10:119
30. Bracaglia C, Prencipe G, De Benedetti F: Macrophage Activation Syndrome: different mechanisms leading to a one clinical syndrome. *Pediatr Rheumatol Online J* 2017; 15:5
31. Jeannet R, Daix T, Formento R, et al.: Severe COVID-19 is associated with deep and sustained multifaceted cellular immunosuppression. *Intensive Care Med* 2020; 46:1769–1771
32. Webb BJ, Peltan ID, Jensen P, et al.: Clinical criteria for COVID-19-associated hyperinflammatory syndrome: a cohort study. *The Lancet Rheumatology* 2020;
33. Moore JB, June CH: Cytokine release syndrome in severe COVID-19. *Science* 2020; 368:473–474
34. Picchianti Diamanti A, Rosado MM, Pioli C, et al.: Cytokine Release Syndrome in COVID-19 Patients, A New Scenario for an Old Concern: The Fragile Balance between Infections and Autoimmunity. *IJMS* 2020; 21:3330–3348
35. Otsuka R, Seino K-I: Macrophage activation syndrome and COVID-19. *Inflamm Regen* 2020; 40:19–6
36. Billiau AD, Roskams T, Van Damme-Lombaerts R, et al.: Macrophage activation syndrome: characteristic findings on liver biopsy illustrating the key role of activated, IFN-gamma-producing

lymphocytes and IL-6- and TNF-alpha-producing macrophages. *Blood* 2005; 105:1648–1651

37. Pinsky MR, Vincent JL, Deviere J, et al.: Serum cytokine levels in human septic shock. Relation to multiple-system organ failure and mortality. *Chest* 1993; 103:565–575
38. Abraham E, Anzueto A, Gutierrez G, et al.: Double-blind randomised controlled trial of monoclonal antibody to human tumour necrosis factor in treatment of septic shock. NORASEPT II Study Group. *The Lancet* 1998; 351:929–933
39. Feldmann M, Maini RN, Woody JN, et al.: Trials of anti-tumour necrosis factor therapy for COVID-19 are urgently needed Comment. *The Lancet* 2020; 1–4
40. Klok FA, Kruip MJHA, van der Meer NJM, et al.: Confirmation of the high cumulative incidence of thrombotic complications in critically ill ICU patients with COVID-19: An updated analysis. *Thromb Res* 2020; 191:148–150
41. Thomas W, Varley J, Johnston A, et al.: Thrombotic complications of patients admitted to intensive care with COVID-19 at a teaching hospital in the United Kingdom. *Thromb Res* 2020; 191:76–77
42. Lodigiani C, Iapichino G, Carenzo L, et al.: Venous and arterial thromboembolic complications in COVID-19 patients admitted to an academic hospital in Milan, Italy. *Thromb Res* 2020; 191:9–14
43. Llitjos J-F, Leclerc M, Chochois C, et al.: High incidence of venous thromboembolic events in anticoagulated severe COVID-19 patients. *J Thromb Haemost* 2020; 18:1743–1746
44. Carsana L, Sonzogni A, Nasr A, et al.: Pulmonary post-mortem findings in a series of COVID-19 cases from northern Italy: a two-centre descriptive study. *The Lancet Infectious Diseases* 2020;
45. Menter T, Haslbauer JD, Nienhold R, et al.: Postmortem examination of COVID-19 patients reveals diffuse alveolar damage with severe capillary congestion and variegated findings in lungs and other organs suggesting vascular dysfunction. *Histopathology* 2020; 47:234
46. Lax SF, Skok K, Zechner P, et al.: Pulmonary Arterial Thrombosis in COVID-19 With Fatal Outcome: Results From a Prospective, Single-Center, Clinicopathologic Case Series. *Ann Intern Med* 2020; M20–2566
47. Goshua G, Pine AB, Meizlish ML, et al.: Endotheliopathy in COVID-19-associated coagulopathy: evidence from a single-centre, cross-sectional study. [Internet]. *Lancet Haematol* 2020; Available from: http://eutils.ncbi.nlm.nih.gov/entrez/eutils/elink.fcgi?dbfrom=pubmed&id=32619411&retmode=ref&cmd=prlinks
48. Saito Y, Kondo H, Hojo Y: Granzyme B as a novel factor involved in cardiovascular diseases. *J Cardiol* 2011; 57:141–147
49. Shaver CM, Upchurch CP, Janz DR, et al.: Cell-free hemoglobin: a novel mediator of acute lung injury. *Am J Physiol Lung Cell Mol Physiol* 2016; 310:L532–41
50. Lowrey AJ, Cramblet W, Bentz GL: Viral manipulation of the cellular sumoylation machinery. *Cell Commun Signal* 2017; 15:27
51. Chiaretti A, Ferrara P, Barone G, et al.: Circulating Plasma Levels of Neurotrophins are Increased in Children with H1N1 Virus Infection. *J Cell Sci Ther* 2013; 4

52. Prakash YS, Martin RJ: Brain-derived neurotrophic factor in the airways. *Pharmacol Ther* 2014; 143:74–86
53. Li Y-C, Bai W-Z, Hashikawa T: The neuroinvasive potential of SARS-CoV2 may play a role in the respiratory failure of COVID-19 patients. *J Med Virol* 2020; 92:552–555
54. Shu T, Ning W, Wu D, et al.: Plasma Proteomics Identify Biomarkers and Pathogenesis of COVID-19. *Immunity* 2020; 53:1–15

Tables

Table 1: Subject demographics and clinical data.

Variable	COVID19+ Patients	COVID19– Patients	P-value
n	7	7	1.000
Age in years	60.0 (56.0, 67.0)	60.0 (53.0, 63.0)	0.520
Sex	5F:2M	5F:2M	1.000
MODS	4.0 (1.0, 7.0)	5.0 (3.0, 7.0)	0.400
SOFA	4.0 (3.0, 9.0)	5.0 (4.0, 11.0)	0.334
Comorbidities, n (%)			
Hypertension	4 (57.1)	6 (85.7)	0.559
Diabetes	2 (28.6)	3 (42.9)	1.000
Chronic kidney disease	1 (14.3)	0 (0)	1.000
Cancer	1 (14.3)	1 (14.3)	1.000
Admission Laboratory Values			
WBC (x 10^9/L)	8.2 (3.8, 12.9)	19.3 (13.6, 24.8)	0.018*
Neutrophils (x 10^9/L)	7.3 (3.8, 11.1)	13.0 (11.7, 22.2)	0.025*
Lymphocytes (x 10^9/L)	0.7 (0.6, 1.0)	1.4 (0.4, 1.7)	0.608
Platelets (x 10^9/L)	202 (119, 225)	212 (145, 291)	0.565
Hemoglobin (g/L)	122 (104, 137)	123 (98, 137)	0.898
Creatinine (µmol/L)	68 (45, 184)	65 (49, 80)	0.609
P:F ratio	124 (69, 202)	172 (132, 304)	0.317
Admission Chest X-ray findings, n (%)			
Bilateral pneumonia	7 (100)	1 (14.3)	0.005*
Unilateral pneumonia	0 (0)	4 (57.1)	0.070
Interstitial infiltrates	0 (0)	1 (14.3)	1.000
Normal	0 (0)	1 (14.3)	1.000
Sepsis diagnosis			
Suspected	0 (0)	4 (57.1)	0.070
Confirmed	7 (100)	3 (42.9)	0.070

Interventions during study			
Antibiotics	7 (100)	7 (100)	1.000
Anti-virals	3 (42.9)	0 (0)	0.192
Steroids	1 (14.3)	2 (28.6)	1.000
Vasoactive medications	5 (71.4)	5 (71.4)	1.000
Renal replacement therapy	1 (14.3)	0 (0)	1.000
High-flow nasal cannula	3 (42.9)	1 (14.3)	0.559
Non-invasive mechanical ventilation	4 (57.1)	7 (100)	0.192
Invasive mechanical ventilation	5 (71.4)	6 (85.7)	1.000
ICU Outcome			
Survived	5 (71.4)	7 (100)	0.462

Continuous data are presented as medians (IQRs). MODS = Multiple Organ Dysfunction Score, SOFA= Sequential Organ Failure Assessment Score, COPD = Chronic Obstructive Pulmonary Disease, WBC = White Blood Cell.

Figures

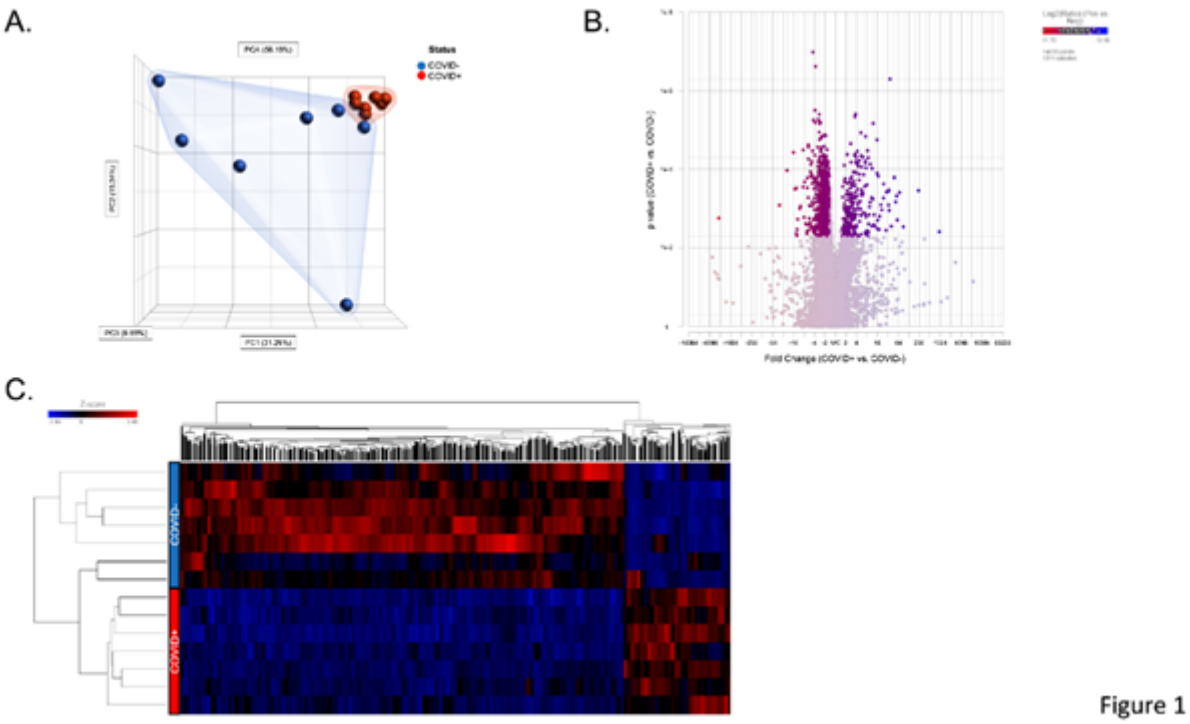

Figure 1

Figure 1

Leukocytes from COVID19+ ICU patients have a unique transcriptional profile compared to leukocytes from COVID19- ICU patients. (A) Principal Component Analysis (PCA) plot of total leucocyte (buffy coat) RNA samples derived from COVID19 positive (COVID+) and negative (COVID-) patients after removing the batch effect of date and interaction between date and status, using all principal components and features contributing equally. (B) Volcano plot of 1,311 genes (highlighted) differentially expressed between leucocyte RNA samples derived from COVID19 positive (COVID+) versus negative (COVID-) samples based on a filtering criterion of +/- 1.5 fold change and an FDR step-up p-value cut off □ 0.0545. (C) Heat map of 1,311 genes that were differentially expressed between leucocyte RNA samples derived from COVID19 positive (COVID+) versus negative (COVID-) samples using average linkage, Euclidean distance metric and standardize normalization mode (shift mean to 0 and scale standard deviation to 1 on all features).

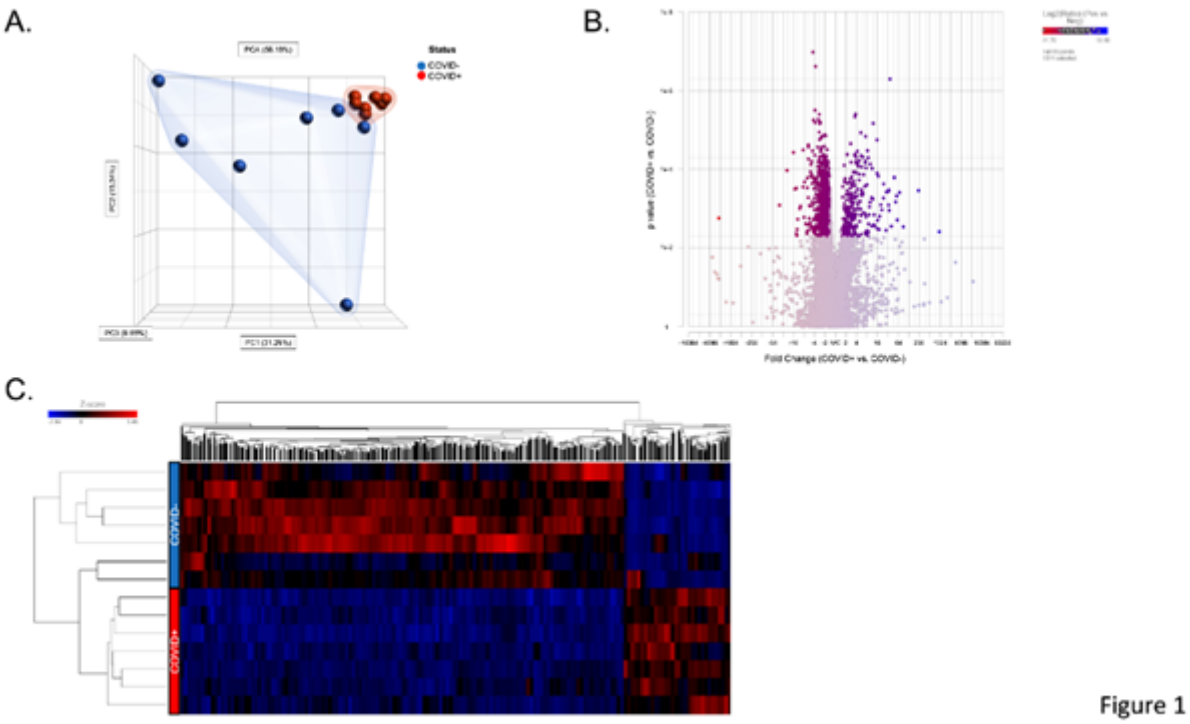

Figure 1

Leukocytes from COVID19+ ICU patients have a unique transcriptional profile compared to leukocytes from COVID19- ICU patients. (A) Principal Component Analysis (PCA) plot of total leucocyte (buffy coat) RNA samples derived from COVID19 positive (COVID+) and negative (COVID-) patients after removing the batch effect of date and interaction between date and status, using all principal components and features contributing equally. (B) Volcano plot of 1,311 genes (highlighted) differentially expressed between leucocyte RNA samples derived from COVID19 positive (COVID+) versus negative (COVID-) samples based on a filtering criterion of +/- 1.5 fold change and an FDR step-up p-value cut off □ 0.0545. (C) Heat map of 1,311 genes that were differentially expressed between leucocyte RNA samples derived from COVID19 positive (COVID+) versus negative (COVID-) samples using average linkage, Euclidean distance metric and standardize normalization mode (shift mean to 0 and scale standard deviation to 1 on all features).

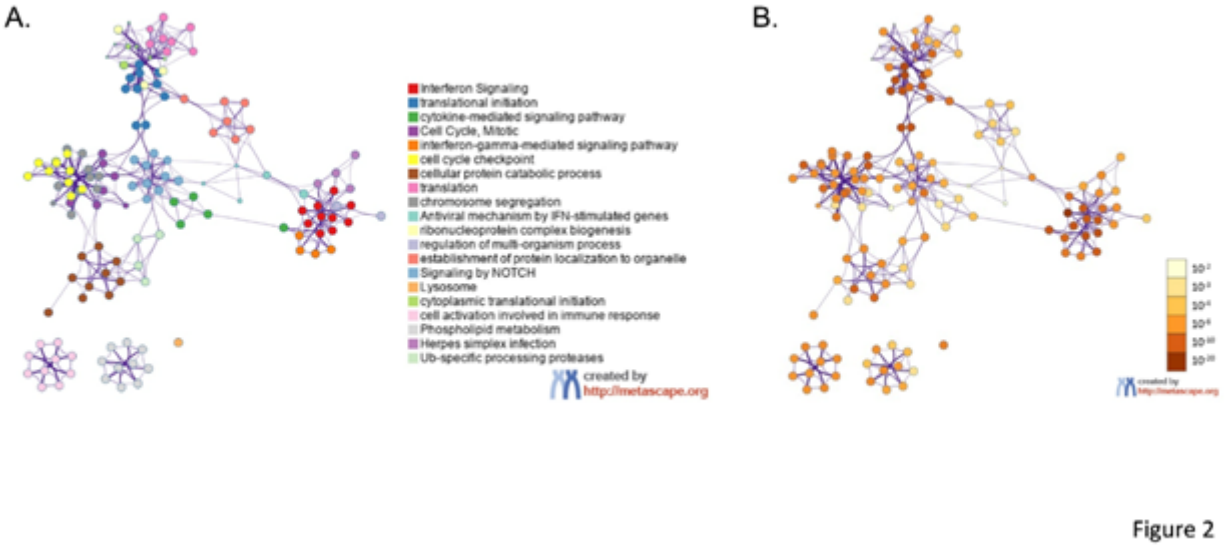

Figure 2

Figure 2

Metascape functional analysis of transcriptional differences in circulating leukocytes from COVID19+ and COVID19- critically ill patients. The list of 1,311 differentially expressed genes was submitted to Metascape using express analysis of Homo sapiens gene IDs. A subset of enriched terms was selected and rendered as a network plot, where terms with a similarity > 0.3 were connected by edges. The network was visualized using Metascape. Each node represents an enriched term and colored first by its cluster ID (A) and then by its p-value (B).

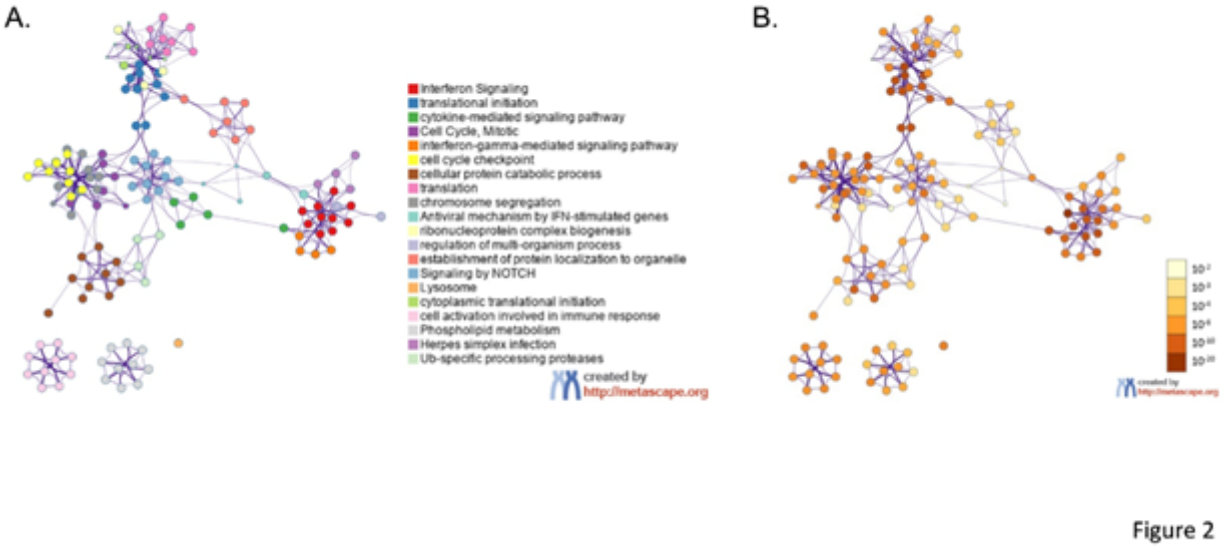

Figure 2

Figure 2

Metascape functional analysis of transcriptional differences in circulating leukocytes from COVID19+ and COVID19- critically ill patients. The list of 1,311 differentially expressed genes was submitted to Metascape using express analysis of Homo sapiens gene IDs. A subset of enriched terms was selected and rendered as a network plot, where terms with a similarity > 0.3 were connected by edges. The network was visualized using Metascape. Each node represents an enriched term and colored first by its cluster ID (A) and then by its p-value (B).

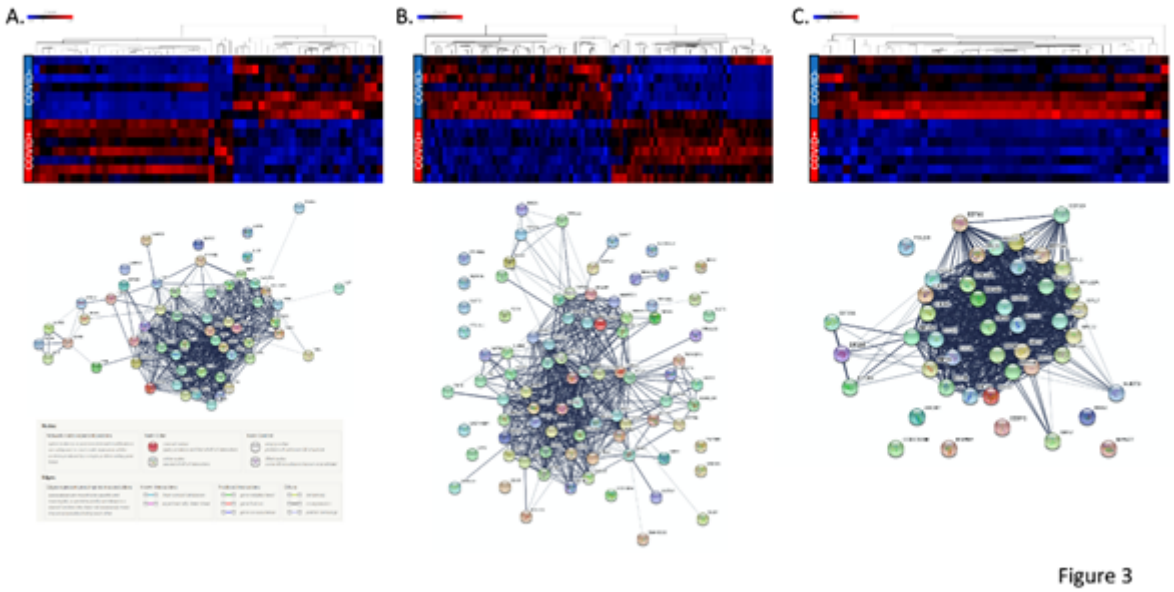

Figure 3

Figure 3

Gene expression and predicted protein-protein interaction networks of transcriptional differences in circulating leukocytes from COVID19+ and COVID19- critically ill patients. Differentially expressed genes (1,311) were submitted to the Reactome Pathway Browser, resulting in the identification of three major pathway classifications (shown as heat maps, left to right): (A) Interferon (Interferon Signalling, Interferon alpha/beta signalling, Antiviral mechanism by IFN-stimulated genes); (B) Cell Cycle Regulation (Cell Cycle, Mitotic, G1/S Transition, Mitotic G1 phase and G1/S transition, G1/S-Specific Transcription); and (C) Protein Translation/Ribosomes (GTP hydrolysis and joining of the 60S ribosomal subunit, Formation of a pool of free 40S subunits, Formation of the ternary complex, the 43S complex, Eukaryotic Translation Initiation, Cap-dependent Translation Initiation, L13a-mediated translational silencing of Ceruloplasmin expression, Eukaryotic Translation Elongation, Peptide chain elongation, Translation initiation complex formation, Response of EIF2AK4 (GCN2) to amino acid deficiency). The gene lists corresponding to these three pathway classifications were submitted to String-db (https://string-db.org/cgi/input.pl) to predict the protein-protein interaction networks (shown below each corresponding heat map).

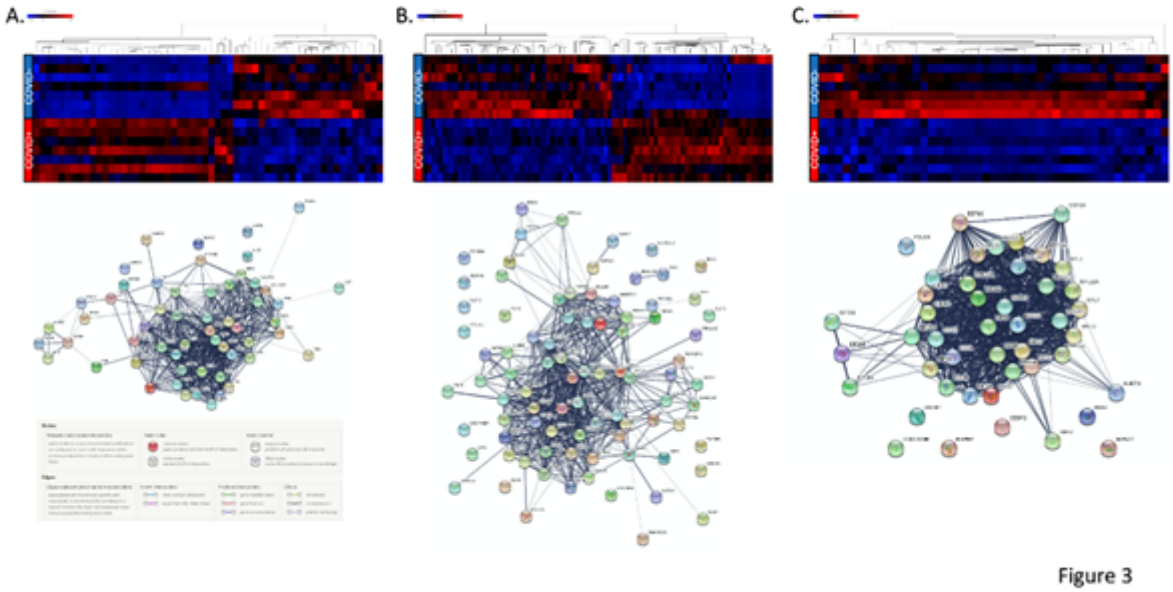

Figure 3

Figure 3

Gene expression and predicted protein-protein interaction networks of transcriptional differences in circulating leukocytes from COVID19+ and COVID19- critically ill patients. Differentially expressed genes (1,311) were submitted to the Reactome Pathway Browser, resulting in the identification of three major pathway classifications (shown as heat maps, left to right): (A) Interferon (Interferon Signalling, Interferon alpha/beta signalling, Antiviral mechanism by IFN-stimulated genes); (B) Cell Cycle Regulation (Cell Cycle, Mitotic, G1/S Transition, Mitotic G1 phase and G1/S transition, G1/S-Specific Transcription); and (C) Protein Translation/Ribosomes (GTP hydrolysis and joining of the 60S ribosomal subunit, Formation of a pool of free 40S subunits, Formation of the ternary complex, the 43S complex, Eukaryotic Translation Initiation, Cap-dependent Translation Initiation, L13a-mediated translational silencing of Ceruloplasmin expression, Eukaryotic Translation Elongation, Peptide chain elongation, Translation initiation complex formation, Response of EIF2AK4 (GCN2) to amino acid deficiency). The gene lists corresponding to these three pathway classifications were submitted to String-db (https://string-db.org/cgi/input.pl) to predict the protein-protein interaction networks (shown below each corresponding heat map).

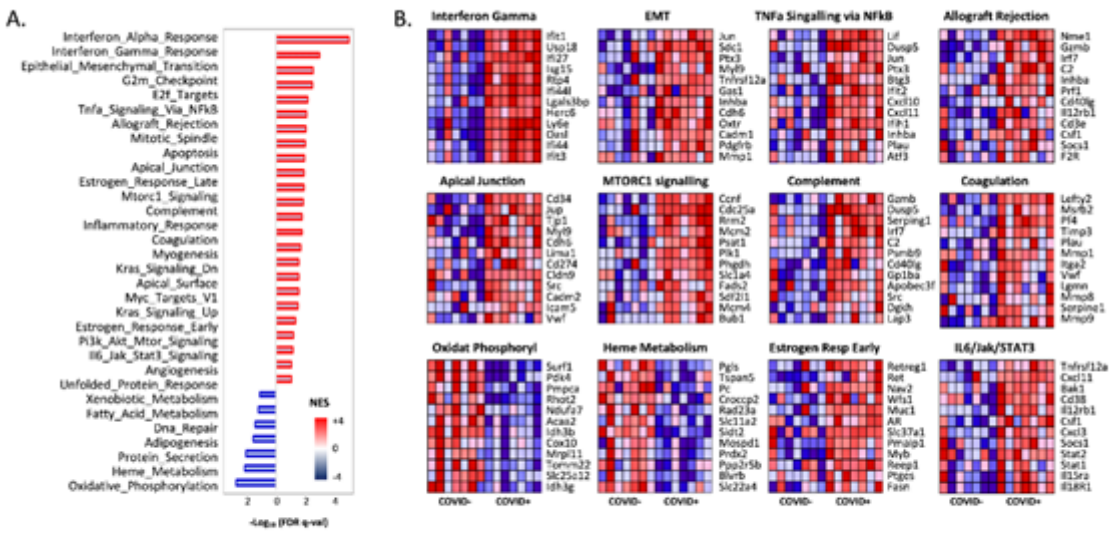

Figure 4

Figure 4

Gene Set Enrichment Analysis of transcriptional differences in circulating leukocytes from COVID19+ and COVID19- critically ill patients. (A) Histogram of Hallmark gene set enrichment analysis. A total of 26/50 gene sets were positively enriched in the phenotype COVID positive (+) and 7/50 gene sets showed positive enrichment for the COVID negative (-) phenotype. Differentially regulated gene sets were ranked by Normalized Enrichment Score (NES) and plotted against the – Log10 of the false discovery rate (FDR q value). (B) Heat maps of the top 12 gene sets in the ranking list in A. Red indicates positive enrichment and blue indicates negative enrichment of gene transcripts.

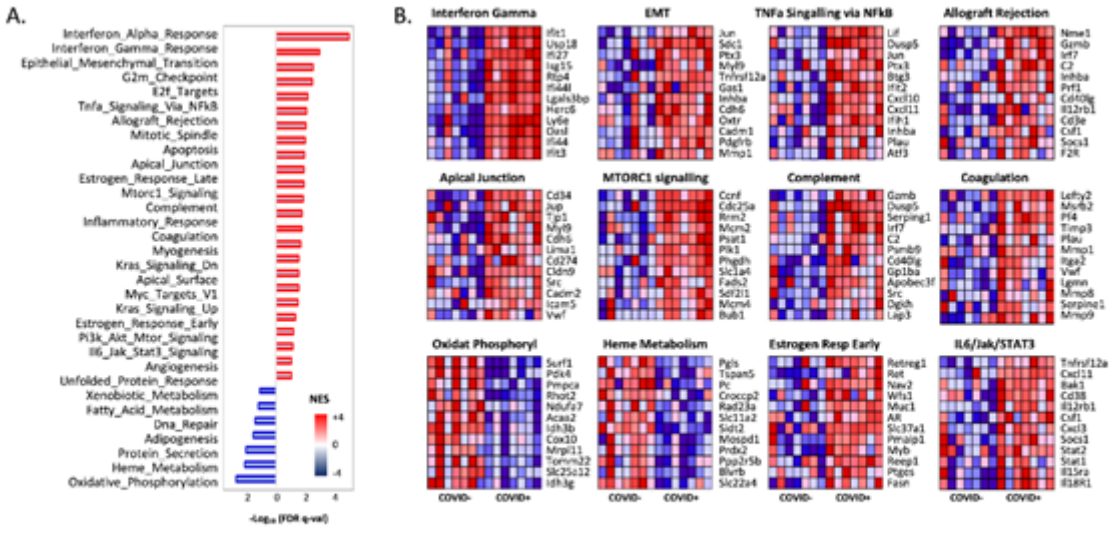

Figure 4

Figure 4

Gene Set Enrichment Analysis of transcriptional differences in circulating leukocytes from COVID19+ and COVID19- critically ill patients. (A) Histogram of Hallmark gene set enrichment analysis. A total of 26/50 gene sets were positively enriched in the phenotype COVID positive (+) and 7/50 gene sets showed positive enrichment for the COVID negative (-) phenotype. Differentially regulated gene sets were ranked by Normalized Enrichment Score (NES) and plotted against the – Log10 of the false discovery rate (FDR q value). (B) Heat maps of the top 12 gene sets in the ranking list in A. Red indicates positive enrichment and blue indicates negative enrichment of gene transcripts.

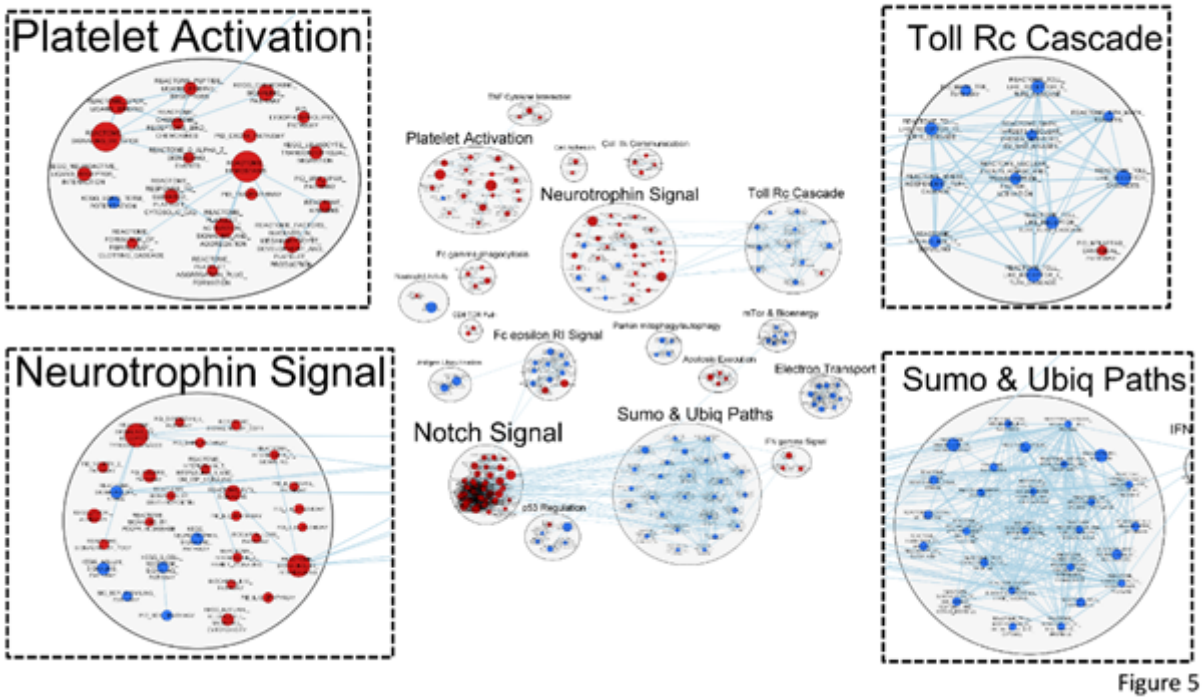

Figure 5

Correlation network generated from transcriptional differences in circulating leukocytes derived from COVID19+ and COVID19- critically ill patients. Each node represents a unique gene-set and the edges represent the coefficient of similarity between gene-sets above a defined threshold. Markov Cluster Algorithm (MCL) clustering analyses revealed groups of gene transcript nodes, where platelet activation, Neurotrophin signalling, Toll-like Receptor signalling cascades, and Sumoylation/ubiquitination pathways were identified as the top four nodes. Red indicates positive enrichment of gene transcripts and blue indicates negative enrichment of gene transcripts.

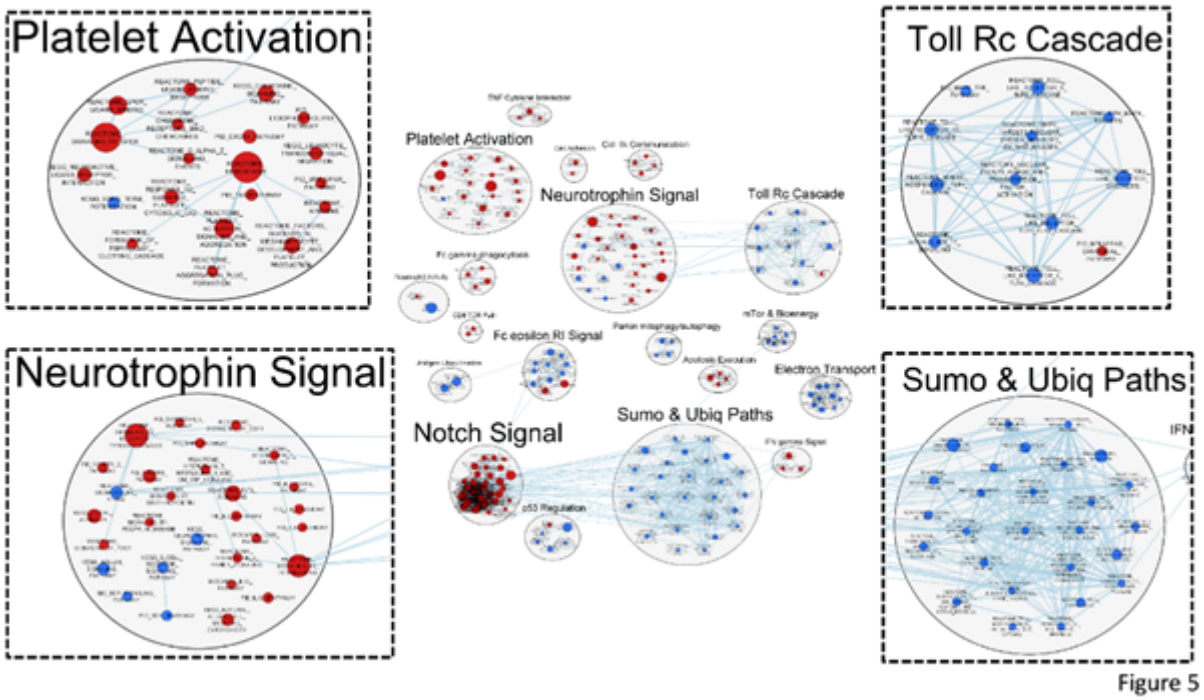

Figure 5

Correlation network generated from transcriptional differences in circulating leukocytes derived from COVID19+ and COVID19- critically ill patients. Each node represents a unique gene-set and the edges represent the coefficient of similarity between gene-sets above a defined threshold. Markov Cluster Algorithm (MCL) clustering analyses revealed groups of gene transcript nodes, where platelet activation, Neurotrophin signalling, Toll-like Receptor signalling cascades, and Sumoylation/ubiquitination pathways were identified as the top four nodes. Red indicates positive enrichment of gene transcripts and blue indicates negative enrichment of gene transcripts.

Supplementary Files

This is a list of supplementary files associated with this preprint. Click to download.

- FigS1.png
- FigS1.png
- FigS2.png
- FigS2.png
- FigS3.png
- FigS3.png
- FigS4.png

- FigS4.png
- RNASupplementalTable2ver2.docx
- RNASupplementalTable2ver2.docx
- RNASupplementalTable1.docx
- RNASupplementalTable1.docx